A New Distributed Energy System with Advanced Utilization of Internal Combustion Engine Waste Heat

Jun Sui, Hao Liu, Feng Liu, and Wei Han

***Abstract*—A new trigeneration system which consists of an internal combustion engine, a power and cooling cogeneration system and an absorption heat transformer system is proposed in this work. The exhaust gas is recovered by the power and cooling cogeneration subsystem producing the cooling and power. The jacket water is recovered by the absorption heat transformer subsystem producing low-pressure steam. The exergy performance and the energy saving performance which is evaluated by the primary energy saving ratio of the new distributed energy system are analyzed. The effects of the ratio of the output power and cooling of the power and cooling cogeneration subsystem and the generator outlet temperature of the absorption heat transformer subsystem to the primary energy saving ratio are considered. The contributions of the subsystems to the primary energy saving ratio are quantified. The maximum primary energy saving ratio of the new distributed energy system is 15.8%, which is 3.9 percentage points higher than that of the conventional distributed energy system due to the cascade utilization of the waste heat from the internal combustion engine.**

***Index Terms*—Cascade utilization of energy, distributed energy, waste heat absorption heat transformer, waste heat power and cooling cogeneration.**

I. Introduction

DISTRIBUTED energy systems can convert 75%–80% of input energy to useful energy due to the trigeneration of power, cooling and heating, so they play an important role in energy conservation and greenhouse gas emission reduction. A number of researchers have analyzed and optimized the distributed combined cooling heating and power systems [1].

Internal combustion engines, absorption chillers, and waste heat boilers are always used in conventional distributed energy systems. The absorption chillers are driven by the exhaust gas, whose temperature is always higher than 300°C, of the internal combustion engines. The generator temperature of the absorption chillers is approximately 120°C. Thus, the large temperature difference can result in large exergy destruction. Usually, the jacket water is cooled by the environment or used to directly supply heat.

Due to the small temperature difference between the exhaust gas and the working fluid, a power and cooling cogeneration system is used with the aim of reducing the exergy destruction of the exhaust gas utilization process. References [2] and [3] first proposed a power and cooling cogeneration system whose working fluid was an ammonia-water mixture. The system could utilize heat sources at 100–200°C. References [4]–[11] investigated power and cooling cogeneration systems using heat sources at 257–450°C. The exergy efficiencies were about 40%. The system in [10] was composed of a Rankine cycle and an absorption refrigeration cycle with the condensation heat of the Rankine cycle as the heat source. The energy saving ratio of the system was 17.1%.

There is great potential for absorption heat transformers to produce hot water and steam when needed. In [12], an absorption heat transformer was used in a power plant to produce steam at a temperature of 140°C. The heat output of the absorption heat transformer is 2.15 MW and the coefficient of performance (COP) is 0.483. The steam extracted from the turbine, whose temperature is 90°C, served as the heat source. In [13], with the purpose of recovering the latent heat of the exhaust gas from a furnace in a municipal waste treatment plant, a vertical absorption heat transformer was used to produce low-pressure steam. In [14]–[16], the heat transformers were used to produce hot water with a COP of about 0.4. In [17] and [18], the heat transformers were integrated into power generation systems. As a result, the system efficiencies increased by less than 10%.

In the distributed CCHP systems, driven by an internal combustion engine in an industrial park where both cooling and low-pressure steam are needed, power and cooling cogeneration systems and absorption heat transformers can be integrated into the systems. This work established a distributed energy system like this and analyzed the exergy and energy saving performances.

II. Description of the Proposed New System

The schematic configuration of the proposed system is shown in Fig. 1, which consists of an internal combustion engine (ICE) subsystem, a power and cooling cogeneration (PCC) subsystem, and an absorption heat transformer (AHT) subsystem. The exhaust gas of the ICE subsystem is sent to

Manuscript received December 8, 2015; revised April 14, 2016 and October 1, 2016; accepted February 21, 2017. Date of publication March 30, 2017; date of current version August 10, 2017. This work was supported in part by the National Basic Research Program of China (No. 2014CB249202), International Science & Technology Cooperation Program of China (No. S2014GR03880).

J. Sui (corresponding author, e-mail: suijun@iet.cn), H. Liu , F. Liu, and W. Han are with the Institute of Engineering Thermophysics, Chinese Academy of Sciences, Beijing, 100190 China.

DOI: 10.17775/CSEEJPES.2015.01260

the waste heat boiler of the PCC subsystem and then discharged into the environment. The schematic configuration of the PCC subsystem is shown in Fig. 2. The subsystem is composed of a Rankine cycle and an absorption refrigeration cycle. The superheated vapor from the waste heat boiler is sent to a turbine to produce power and then to a rectifier as a heat source. The vapor from the rectifier is condensed in a condenser and driven back to the waste heat boiler. The refrigerant that is generated from the rectifier is condensed in a condenser, cooled in a regenerator and then sent to a valve. The refrigerant from the valve is sent to an evaporator to produce cooling. Then, the refrigerant is heated in the regenerator and sent to an absorber. The weak solution from the rectifier is also sent to the absorber through a solution heat exchanger and a valve. The strong solution from the absorber is pumped into the solution heat exchanger and then to the rectifier. The jacket water of the ICE subsystem is successively sent to the evaporator and generator of the AHT subsystem as a heat source. The schematic configuration of the AHT subsystem is shown in Fig. 3. The steam from the generator is sent to a condenser and then pumped into the evaporator. The steam that is evaporated from the evaporator is absorbed in an absorber by the strong solution from a solution heat exchanger and releases heat to produce low-pressure steam. The strong solution from the generator is pumped to the solution heat exchanger and heated by the weak solution from the absorber. At last the weak solution from the solution heat exchanger is sent to a valve and then to the generator.

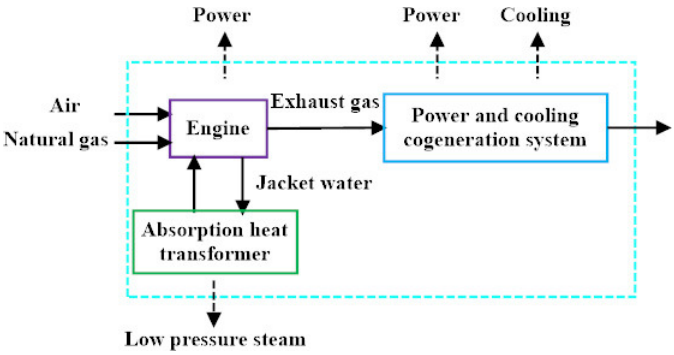

Fig. 1. Schematic configuration of the new system.

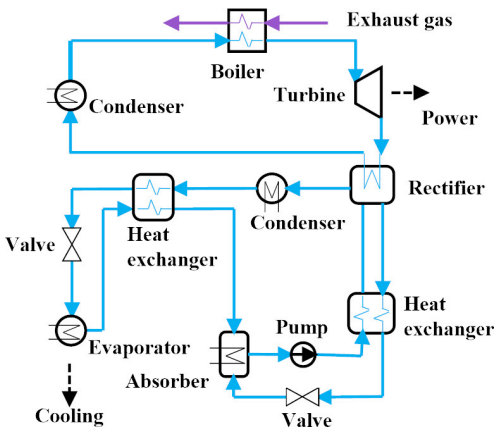

Fig. 2. Schematic configuration of the PCC subsystem.

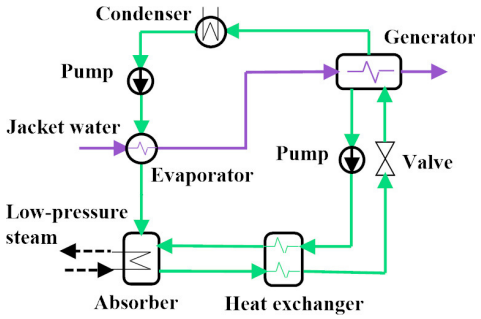

Fig. 3. Schematic configuration of the AHT subsystem.

A conventional CCHP system driven by an internal combustion engine shown in Fig. 4 is selected as the reference system, which is composed of an internal combustion engine subsystem, an absorption refrigerator (AR) subsystem, and a waste heat boiler (WHB) subsystem. The exhaust gas of the ICE subsystem is sent to the rectifier of the AR subsystem as a heat source and then sent to the WHB subsystem to produce low-pressure steam. The jacket water of the ICE subsystem is cooled by the environment in the cooling tower.

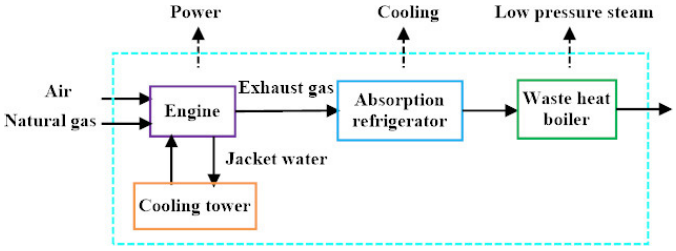

Fig. 4. Schematic configuration of the reference system.

III. System Simulation and Evaluation

A. Simulation Conditions and System Modeling

The simulation conditions of the new system are shown in Table I. The internal combustion engine is a turbocharged six-cylinder spark ignition engine fueled by natural gas and is simulated using the software GTPower. The working fluids of the PCC subsystem and the AHT subsystem are ammonia-water solution and lithium bromide-water solution, respectively. The Rankine cycle of the PCC subsystem is simulated using the software Aspen Plus and the properties of the working fluid is calculated by the Peng-Robinson equation of state. The absorption refrigeration cycle of the PCC subsystem and the AHT subsystem are simulated using the software Engineering Equation Solver. The correlations in [19] are used to calculate the properties of the lithium bromide-water solution. The mathematical models developed in the Engineering Equation Solver are as follows:

Mass conservation:

$$\sum m_{\text{in}} = \sum m_{\text{out}} \tag{1}$$

$$\sum m_{\text{in}} X_{\text{in}} = \sum m_{\text{out}} X_{\text{out}}. \tag{2}$$

Energy conservation:

$$Q = \sum m_{\text{out}} h_{\text{out}} - \sum m_{\text{in}} h_{\text{in}} + W. \tag{3}$$

Phase equilibrium:

$$f(T, P, X) = 0 \tag{4}$$

where m is the mass flow of the working fluids; X is the concentration of solutions; h is the specific enthalpy of the working fluids; Q and W are the input heat and output work of the components, respectively; T and P are the temperature and pressure of the working fluids; the subscript "in" and "out" denote the inlet port and outlet port of the components of the subsystems, respectively.

TABLE I
SIMULATION CONDITIONS OF THE NEW SYSTEM

Simulation Conditions	Value
Environment temperature (°C)	25
Environment pressure (kPa)	100
Internal combustion engine rated power (kW)	64
Internal combustion engine efficiency (%)	36
A/F ratio	32
Compression ratio of the internal combustion engine	12
Maximum temperature of cylinders (°C)	1,648
Jacket water temperature (°C)	86
Jacket water flow rate (kg/s)	0.97
Exhaust gas temperature (°C)	412
Exhaust gas flow rate (kg/s)	0.12
Pinch point temperature difference of waste heat boiler (°C)	20
Thermal efficiency of waste heat boiler (%)	95
Waste heat boiler exhaust gas temperature (°C)	115
Pressure loss of heat exchangers (%)	3
Heat exchanger effectiveness	0.9
Turbine inlet temperature (°C)	390
Turbine inlet pressure (kPa)	2,500
Turbine inlet working fluid concentration (%)	33
Turbine isentropic efficiency (%)	80
Maximum temperature of rectifier (°C)	120
Refrigeration temperature (°C)	−13.7
Maximum temperature of generator (°C)	73
Thermal efficiency of generator (%)	95
Low-pressure steam temperature (°C)	115
Low-pressure steam quality (%)	100
Cooling water temperature (°C)	25

B. Evaluation Criteria

The criteria that were used in this work are the primary energy saving ratio (PESR) and exergy efficiency. The primary energy saving ratio is the ratio of the energy consumption difference (between the distributed energy system and the separate system) and the energy consumption of the separate system given that the output power, cooling, and heating of the distributed energy system are equal to those of the separate system. The schematic diagram for the calculation of the PESR is shown in Fig. 5. In the separate system, the power, cooling, and heating are provided by a power grid (PG), an electric compression refrigerator (ECR), and a gas boiler (GB), respectively. Considering the general situation, the power and heating supply efficiencies in the separate system are 35.8% and 92%, respectively. The COP of the ECR of the separate system is 4.2. The primary energy saving ratio of the new system is compared with that of the reference system to quantify the benefits obtained.

The primary energy saving ratio is calculated by the following equation:

$$R = (E_0 - E)/E_0 \tag{5}$$

where R is the primary energy saving ratio; E_0 is the energy consumption of the separate system, of which the output power, heating, and cooling are equal to those of the distributed energy system; and E is the energy consumption of the distributed energy system. E_0 is calculated as follows:

$$E_0 = W/\eta_{0,\mathrm{e}} + Q_\mathrm{r}/\eta_{0,\mathrm{r}} + Q_\mathrm{h}/\eta_{0,\mathrm{h}} \tag{6}$$

where W, Q_r, and Q_h are the output power, cooling, and heating of the distributed energy system, respectively; $\eta_{0,\mathrm{e}}$ is the power supply efficiency of the separate system; $\eta_{0,\mathrm{r}}$ is the production of the COP of the ECR and power supply efficiency of the separate system; and $\eta_{0,\mathrm{h}}$ is the heat supply efficiency of the separate system.

Substituting (6) into (5) results in:

$$\begin{aligned} R = {} & (W_\mathrm{en}/\eta_{0,\mathrm{e}} - E)/E_0 \\ & + (W_\mathrm{pc}/\eta_{0,\mathrm{e}} + Q_\mathrm{r}/\eta_{0,\mathrm{r}})/E_0 + Q_\mathrm{h}/(\eta_{0,\mathrm{h}} E_0) \end{aligned} \tag{7}$$

where W_en is the output power of the ICE subsystem; W_pc is the output power of the PCC subsystem. To the right side of the equal sign of (7), the first term denotes the contribution to the primary energy saving ratio of the ICE subsystem. The second term denotes the contribution of the PCC subsystem. The third term denotes the contribution of the AHT subsystem.

The exergy efficiency of the waste heat utilization process is calculated by the following equation:

$$\eta_\mathrm{ex} = (W + E_{\mathrm{ex,r}} + E_{\mathrm{ex,h}})/E_{\mathrm{ex,f}} \tag{8}$$

where W is the output power of the waste heat utilization process; $E_{\mathrm{ex,r}}$ is the output cooling exergy of the waste heat utilization process; $E_{\mathrm{ex,h}}$ is the output heating exergy of the waste heat utilization process; and $E_{\mathrm{ex,f}}$ is the exergy of the waste heat.

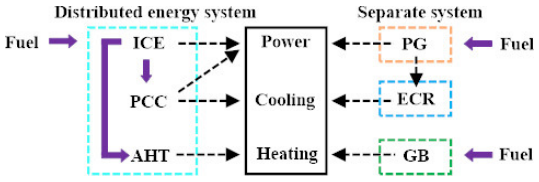

Fig. 5. Primary energy saving ratio calculation schematic diagram.

IV. RESULTS AND DISCUSSION

A. Parametric Analysis and Discussion

1) Effect of the Ratio of the Output Power and Cooling of the PCC Subsystem

It can be seen from (7) that the PESR is closely related to the output power and cooling of the PCC subsystem given that the input energy is constant. So the effect of the ratio of the output power and cooling of the PCC subsystem on the system performance is investigated. The cooling is generated by the absorption refrigeration cycle using the condensation heat of the Rankine cycle, thus the ratio of the output power and cooling is determined by the turbine outlet pressure given that the cooling water temperature is constant. The curve of the PESR versus the ratio of the output power and cooling of the PCC subsystem is shown in Fig. 6. The PESR is 12.5%

when the PCC subsystem produces cooling only due to the low COP of the absorption refrigeration cycle. The PESR increases quickly when the high temperature waste heat is used to produce power. The maximum PESR is 15.8% at a ratio of 0.5. When the ratio is higher than 0.5, the PESR decreases with the increasing ratio in that too much low-temperature heat is released from the condenser to the environment due to the low efficiency of waste heat power generation. The PESR is 15.3% when the PCC subsystem only produces power. The curves of the contributions to the PESR of the subsystems versus the ratio of the output power and cooling of the PCC subsystem are shown in Fig. 7. There exists a maximum value of the contribution of the PCC subsystem and there are no obvious changes of the contributions of the ICE subsystem and the AHT subsystem due to the constant efficiency and jacket water heat of the ICE subsystem and COP of the AHT subsystem.

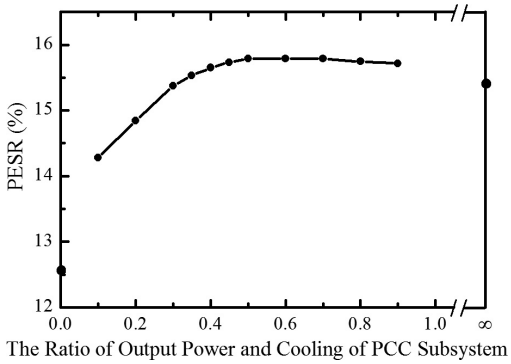

Fig. 6. Diagram of the PESR versus the ratio of output power and cooling of the PCC subsystem.

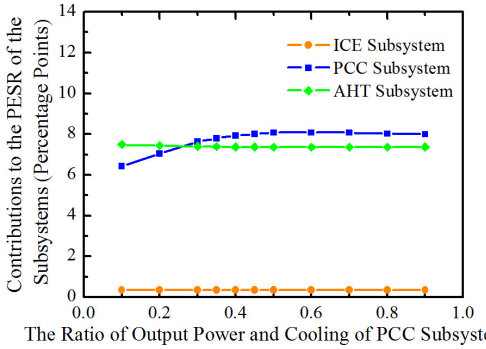

Fig. 7. Diagram of the contributions to the PESR of the subsystems versus the ratio of output power and cooling of the PCC subsystem.

2) Effect of the Generator Outlet Temperature of the AHT Subsystem

The effect of the performance of the AHT subsystem on the system performance is also investigated. The generator outlet temperature can obviously influence the COP of the AHT subsystem and then the PESR of the system. The curves of the COP of the AHT subsystem and the PESR versus the generator outlet temperature of the AHT subsystem are shown in Fig. 8. The COP of the AHT subsystem increases with the increasing generator outlet temperature. The PESR also increases due to the increasing heat produced by the AHT subsystem. The curves of the contributions to the PESR of the subsystems versus the generator outlet temperature of the AHT subsystem are shown in Fig. 9. The contribution of the AHT subsystem increases due to the increasing heat produced. There are no obvious changes of the contributions of the ICE subsystem and the PCC subsystem due to the constant efficiency and exhaust gas heat of the ICE subsystem and the ratio of the output power and cooling of the PCC subsystem.

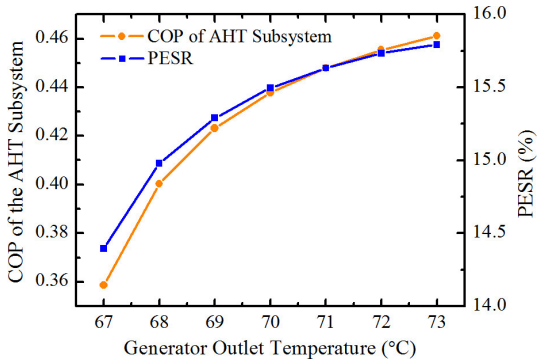

Fig. 8. Diagram of the COP of the AHT subsystem and the PESR versus the generator outlet temperature of the AHT subsystem.

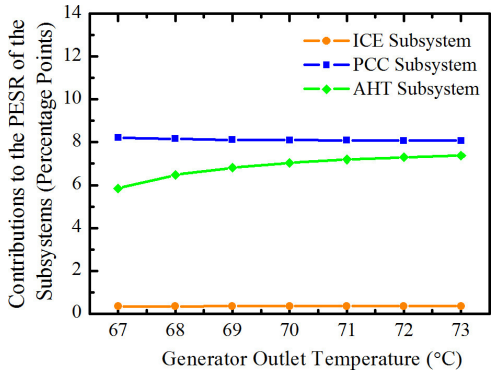

Fig. 9. Diagram of the contributions to the PESR of the subsystems versus the generator outlet temperature of the AHT subsystem.

B. Exergy Analysis

Given that the ratio of the output power and cooling of the PCC subsystem and the generator outlet temperature of the AHT subsystem are 0.5 and 73°C, respectively, the energy performance values of the new system and the reference system are shown in Table II. The PESR values of the new system and the reference system are 15.8% and 11.9%, respectively. The exergy performance values of the waste heat utilization process for the new system and the reference system are shown in Table III. The exergy efficiencies of the waste heat utilization process for the new system and the reference system are 34.4% and 22.2%, respectively.

The differences between the new system and the reference system shown in Table III can be explained with the help of the T-S diagrams of the exhaust gas utilization process of the two systems shown in Fig. 10 and Fig. 11, respectively. The temperature of the exhaust gas, whose temperature is

TABLE II
ENERGY PERFORMANCE OF THE SYSTEMS

Items	New System	Reference System
Input energy (kW)		
Natural gas	176	176
Output energy (kW)		
Power	67.7	63.1
Cooling	7.7	7.7
Heating	14.2	17.5
Energy loss (kW)		
ICE subsystem	8.3	41
PCC subsystem	42.1	
AR subsystem		24.6
AHT subsystem	19.2	
WHB subsystem		1.9
Exhaust gas	32.8	36.2

TABLE III
EXERGY PERFORMANCE OF THE WASTE HEAT UTILIZATION PROCESS

Items	New System	Reference System
Input exergy (kW)		
Exhaust gas (cooled to 115°C)	18.7	18.7
Jacket water	5	5
Output exergy (kW)		
Power exergy	4.2	
Cooling exergy	1.1	1.1
Heating exergy	2.8	4.1
Exergy loss (kW)		
PCC subsystem	13.4	
AR subsystem		10.9
AHT subsystem	3.7	
WHB subsystem		3.9
Jacket water		5
Exergy efficiency (%)	34.4	22.2

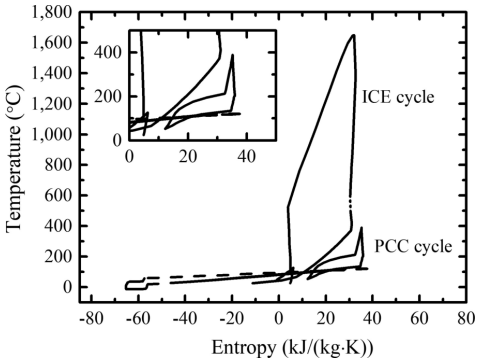

Fig. 10. The T-S diagram of the exhaust gas utilization process of the new system.

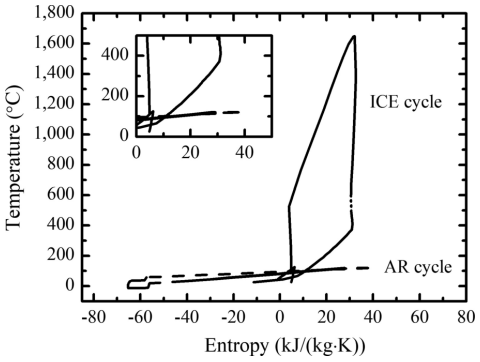

Fig. 11. The T-S diagram of the exhaust gas utilization process of the reference system.

412°C, is 292°C higher than the temperature of the ammonia-water mixture in the rectifier of the AR subsystem of the reference system. And then the exhaust gas from the rectifier, whose temperature is 285°C, is used to heat the production water from 95°C to 115°C in the WHB subsystem. In the new system, the temperature of the exhaust gas is 22°C higher than the temperature of the ammonia-water vapor at the inlet of the turbine of the PCC subsystem. Thus, the smaller temperature difference in the new system compared with that of the reference system results in a nine-percent reduction of exergy destruction. The temperature of the jacket water of the ICE subsystem is 86°C and decreased to 78°C to produce production water in the AHT subsystem of the new system. In the reference system, the jacket water is cooled by the environment. Therefore, the recovery of the jacket water of the new system also results in a 26-percent reduction of exergy destruction. As a result, the exergy loss of the waste heat utilization process of the new system is 13.6% lower than that of the reference system.

C. Primary Energy Saving Ratio Analysis

The contributions to the PESR of the subsystems are shown in Table IV. The ICE subsystem contributes the least to the PESR due to the small efficiency difference between the ICE and power supply of the separate system. In the reference system, the pump power of the AR subsystem is supplied by the ICE subsystem so the output power is reduced and the contribution of the ICE subsystem is negative. There is much power produced using the exhaust gas in the new system, so the contribution of the PCC subsystem is much higher than that of the AR subsystem in the reference system. The AHT subsystem of the new system using the jacket water to produce low-pressure steam contributes 7.4 percentage points to the PESR while the jacket water of the reference system is cooled by the environment.

TABLE IV
CONTRIBUTIONS TO THE PRIMARY ENERGY SAVING RATIO OF THE SUBSYSTEMS

Contributions (percentage points)	NEW SYSTEM	Reference System
ICE subsystem	0.3	−0.2
PCC subsystem	8.1	
AR subsystem		2.6
AHT subsystem	7.4	
WHB subsystem		9.5
Total	15.8	11.9

V. CONCLUSION

A new distributed energy system utilizing a PCC system and AHT system driven by ICE is proposed. The exergy and energy saving performance of the new system is analyzed and the contributions of the subsystems are investigated.

1) The maximum PESR occurs when the ratio of the output power and cooling of the PCC subsystem increases. Power and cooling cogeneration is better than the individual production of power or cooling using the exhaust gas. The PESR can be increased by improving the performance of the AHT subsystem.

2) The exergy efficiency of the waste heat utilization process of the new system is 34.4%, which is 12.2 points higher than that of the reference system. The integration of the PCC subsystem and the recovery of jacket water using the AHT subsystem can improve the exergy efficiency of the system driven by internal combustion engines.
3) The PESR of the new system is 15.8%, which is 3.9 percentage points higher than that of the reference system. The ICE subsystem contributes the least to the PESR. The contribution of the PCC subsystem can be significantly higher than the contribution of producing cooling individually using exhaust gas. The AHT subsystem contributes 7.4 percentage points to the PESR which indicates that there is a lot of potential for the recovery of jacket water to produce low-pressure steam.

REFERENCES

[1] H. Cho, A. D. Smith, and P. Mago, "Combined cooling, heating and power: A review of performance improvement and optimization," *Applied Energy*, vol. 136, pp. 168–185, Dec. 2014.

[2] D. Y. Goswami, "Solar thermal power technology: Present status and ideas for the future," *Energy Sources*, vol. 20, no. 2, pp. 137–145, Aug. 1998.

[3] D. Y. Goswami and F. Xu, "Analysis of a new thermodynamic cycle for combined power and cooling using low and mid temperature solar collectors," *Journal of Solar Energy Engineering*, vol. 121, no. 2, pp. 91–97, May 1999.

[4] D. X. Zheng, B. Chen, Y. Qi, and H. G. Jin, "Thermodynamic analysis of a novel absorption power/cooling combined-cycle," *Applied Energy*, vol. 83, no. 4, pp. 311–323, Apr. 2006.

[5] N. Zhang and N. Lior, "Methodology for thermal design of novel combined refrigeration/power binary fluid systems," *International Journal of Refrigeration*, vol. 30, no. 6, pp. 1072–1085, Sep. 2007.

[6] M. Liu and N. Zhang, "Proposal and analysis of a novel ammonia–water cycle for power and refrigeration cogeneration," *Energy*, vol. 32, no. 6, pp. 961–970, Jun. 2007.

[7] N. Zhang and N. Lior, "Development of a novel combined absorption cycle for power generation and refrigeration," *Journal of Energy Resources Technology*, vol. 129, no. 3, pp. 254–265, Sep. 2007.

[8] J. F. Wang, Y. P. Dai, and L. Gao, "Parametric analysis and optimization for a combined power and refrigeration cycle," *Applied Energy*, vol. 85, no. 11, pp. 1071–1085, Nov. 2008.

[9] C. P. Jawahar, R. Saravanan, J. C. Bruno, and A. Coronas, "Simulation studies on gax based Kalina cycle for both power and cooling applications," *Applied Thermal Engineering*, vol. 50, no. 2, pp. 1522–1529, Feb. 2013.

[10] L. L. Sun, W. Han, X. Y. Jing, D. X. Zheng, and H. G. Jin, "A power and cooling cogeneration system using mid/low-temperature heat source," *Applied Energy*, vol. 112, no. 4, pp. 886–897, Dec. 2013.

[11] L. L. Sun, W. Han, D. X. Zheng, and H. G. Jin, "Assessment of an ammonia-water power/cooling cogeneration system with adjustable solution concentration," *Applied Thermal Engineering*, vol. 61, no. 2, pp. 443–450, Nov. 2013.

[12] C. Mostofizadeh and C. Kulick, "Use of a new type of heat transformer in process industry," *Applied Thermal Engineering*, vol. 18, no. 9-10, pp. 857–874, Sep. 1998.

[13] S. Inoue, S. Yamamoto, T. Furukawa, Y. Wakiyama, and K. Ochi, "Improvement of high-temperature applicability and compactness of a unit of an absorption heat pump," *Heat Recovery System & CHP*, vol. 14, no. 3, pp. 305–314, May 1994.

[14] S. Sekar and R. Saravanan, "Experimental studies on absorption heat transformer coupled distillation system," *Desalination*, vol. 274, no. 1-3, pp. 292–301, Jul. 2011.

[15] A. Huicochea, R. J. Romero, W. Rivera, G. Gutierrez-Urueta, J. Siqueiros, and I. Pilatowsky, "A novel cogeneration system: A proton exchange membrane fuel cell coupled to a heat transformer," *Applied Thermal Engineering*, vol. 50, no. 2, pp. 1530–1535, Feb. 2013.

[16] X. H. Ma, J. B. Chen, S. P. Li, Q. Y. Sha, A. M. Liang, W. Li, J. Y. Zhang, G. J. Zheng, and Z. H. Feng, "Application of absorption heat transformer to recover waste heat from a synthetic rubber plant," *Applied Thermal Engineering*, vol. 23, no. 7, pp. 797–806, May. 2003.

[17] V. Zare, M. Yari, and S. M. S. Mahmoudi, "Proposal and analysis of a new combined cogeneration system based on the GT-MHR cycle," *Desalination*, vol. 286, no. 1, pp. 417–428, Feb. 2012.

[18] L. Q. Duan, M. D. Zhao, and Y. P. Yang, "Integration and optimization study on the coal-fired power plant with CO_2 capture using MEA," *Energy*, vol. 45, no. 1, pp. 107–116, Sep. 2012.

[19] Y. Kaita, "Thermodynamic properties of lithium bromide-water solutions at high temperatures," *International Journal of Refrigeration*, vol. 24, no. 5, pp. 374–390, Aug. 2001.

Jun Sui was born in 1973. He received B.S. and M.S. degrees in organic chemical engineering from the Petroleum Institute of Daqing, in 1998, and a Ph.D. in chemical engineering from Dalian University of Technology in 2001, and he was a postdoctoral fellow in heating, gas supply, ventilation and air conditioning at Tsinghua University, in 2003. Since 2003, Jun has served as a Research Assistant, Assistant Professor and Professor at the Institute of Engineering Thermophysics, Chinese Academy of Sciences. His research direction is multi-energy complementary distributed energy systems, which mainly include distributed CCHP technology, absorption heat pump technology, and technology about the complementary use of solar energy and fossil fuels through solar thermal power technology. He was awarded as the Outstanding Technical Personnel in Chinese Academy of Sciences.

Hao Liu received a M.Eng. degree in power engineering from the University of Chinese Academy of Sciences (UCAS), Beijing, China, in 2015. He is now a Ph.D. student at UCAS, and his research direction is distributed CCHP systems.

Feng Liu received a B.S. degree in thermal energy and power engineering from China University of Petroleum, Qingdao, China, in 2007. He is currently pursuing a Ph.D. degree in engineering thermophysics from the University of Chinese Academy of Sciences. His research interests include the absorption heat pump and combined cooling heating and power.

Wei Han received a Ph.D. in engineering thermophysics from Institute of Engineering Thermophysics, Chinese Academy of Sciences, China, in 2006.

From 2006 to 2009, he was a Research Assistant with the Institute of Engineering Thermophysics, CAS. Since 2010, he has been an Associate Professor at the same institute. His research interests include the development of power and cooling cogeneration technologies using surplus heat, the integration of advanced energy systems, and the analysis and optimization of distributed energy systems.

Dr. Han's awards and honors include the 2007 Best Technical Paper Award at the ASME IGTI conference, the 2007 Young Scientists Award at the 20th international conference on ECOS, and the Journal of Applied Energy Outstanding Reviewer of 2010.